Appendix A. Supporting information

Title: Saliva-based COVID-19 detection: a rapid antigen test of SARS-CoV-2 nucleocapsid protein using an electrical-double-layer gated field-effect transistor-based biosensing system

Author names and affiliation: Pin-Hsuan Chen[a,+], Chih-Cheng Huang[b,+], Chia-Che Wu[b], Po-Hsuan Chen[b], Adarsh Tripathi[c], and Yu-Lin Wang[a,b,*]

[a] Department of Power Mechanical Engineering, National Tsing Hua University, Hsinchu 300044, Taiwan (R.O.C.)

[b] Institute of Nanoengineering and Microsystems, National Tsing Hua University, Hsinchu, 300044, Taiwan (R.O.C.)

[c] Institute of Molecular Medicine, National Tsing Hua University, Hsinchu 300044, Taiwan (R.O.C.)

[+] These authors contributed equally to this work.

[*] **Corresponding author**: Yu-Lin Wang. Email: ylwang@mx.nthu.edu.tw

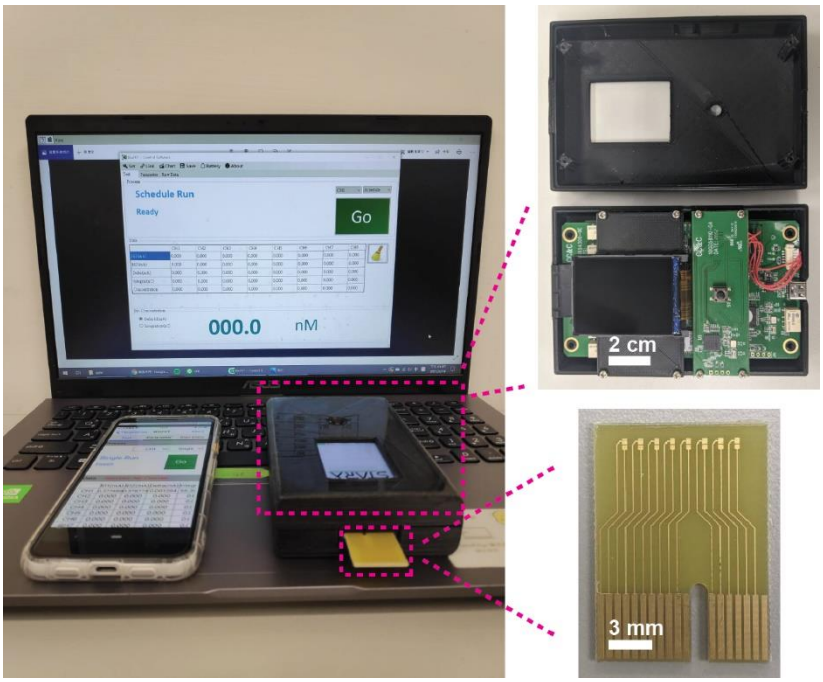

Supplemental Figure 1. Photographs of the system (left) and zoomed-in views (right) of a reader and a sensor stick. The portable testing setup shows the EDL-gated BioFET system, and measurements were recorded through a custom- written user interface as shown on a laptop screen and an iPhone.

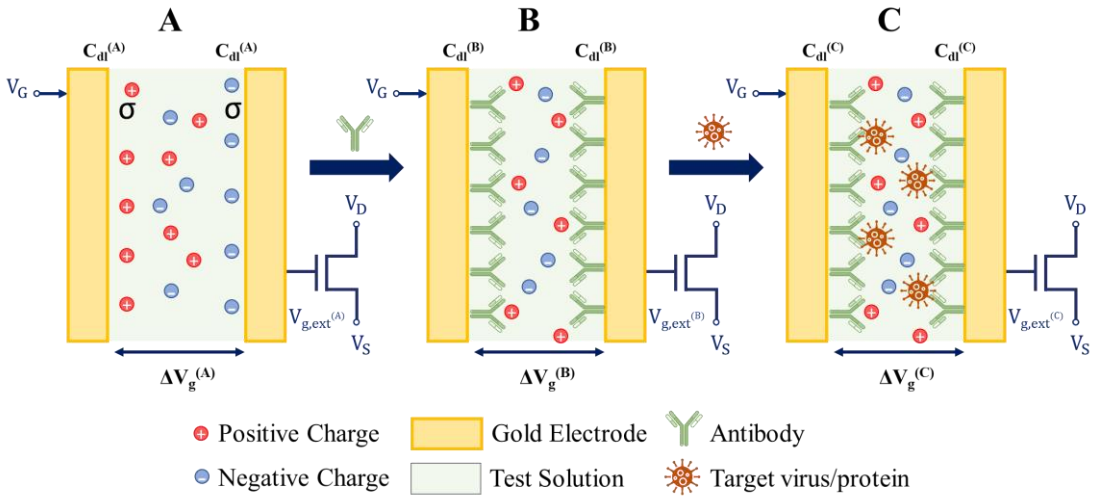

Supplemental Figure 2. Schematic illustrations of sensing principles using an EDL-gated BioFET. Phase A: bare electrodes without functionalization, Phase B: surface modification with capture antibody, and Phase C: target virus/protein bound on capture antibody. The EDL capacitance varies at each phase due to the electrical immuno-respsonse.

Sensing mechanism of an EDL-gated BioFET

The Gouy-Chapman-Stern model was adopted to establish the sensing principle of an EDL-gated BioFET [1]. The EDL structure, which gives rise to a capacitance on a surface, is composed of two layers: the Stern layer and the diffusive layer. The EDL capacitance (C_{dl}) can be written as [2,3]:

$$\frac{1}{C_{dl}} = \frac{1}{C_{Stern}} + \frac{1}{C_{diff}}, \text{ with} \quad \text{(S1)}$$

$$C_{Stern} = \frac{\varepsilon_{r,stern}\varepsilon_0 A}{l_{stern}}, \text{ and} \quad \text{(S2)}$$

$$C_{diff} = \frac{\varepsilon_r \varepsilon_0 A}{l_{diff}}, \quad \text{(S3)}$$

where the C_{Stern} is the capacitance of the Stern layer, C_{diff} is the capacitance of a diffusive layer, l_{stern} is the thickness of Stern layer, ε_0 is the permittivity in vacuum, $\varepsilon_{r,stern}$ is the relative permittivity, A is the surface area of an electrode, l_{diff} is the thickness of a diffusive layer nearly equal to the equivalent thickness of the parallel-plate capacitor, and ε_r is the relative permittivity of a diffusive layer. The thickness of a diffusive layer is usually considered as the Debye length.

The surface charge density (σ_0) is assumed to be equal to the EDL charge density (σ_{dl}) with the same number of opposite charges, written as [4]:

$$\sigma_{dl} = -\sigma_0 = -C_{dl} \cdot \varphi_0, \quad \text{(S4)}$$

where φ_0 is the surface potential defined as the difference between the potential of an electrode surface and the potential of the bulk solution. The Grahame equation can be used to show the relationship between σ_0 and φ_0 [3,5]:

$$\sigma_{dl} = \sqrt{8c_0 \varepsilon \varepsilon_0 K_B T} \cdot sinh\left(\frac{e\varphi_1}{2k_B T}\right), \quad \text{(S5)}$$

where c_0, ε, K_B, T, e and φ_1 represent the ion concentration of the electrolyte, the relative permittivity of the buffer, the Boltzmann constant, the absolute temperature, the elementary electric charge, and the potential at Stern plane, respectively.

The EDL is formed on an electrode due to the charge redistribution while voltage bias is applied. As the antibody is immobilized (**Supplemental Fig. 2**), the EDL is redistributed and a new EDL capacitance (${C_{dl}}^{(B)}$) forms. At Phase C, the antigen is captured by the antibody, forming another capacitance (${C_{dl}}^{(c)}$).

Eq. S6 exhibits the relationship between the gate bias (V_G) and the remaining voltage on the extended electrode at phase i (${V_{g,ext}}^{(i)}$). $\Delta {V_g}^{(i)}$ represents the potential drop/increase across the testing solution, which is dependent on ${C_{dl}}^{(i)}$.

$$V_G + \Delta {V_g}^{(i)} = {V_{g,ext}}^{(i)}. \quad \text{(S6)}$$

The output drain current (I_d) gets affected due to the changes of $V_{g,ext}$, determining how much potential change occurred on a testing sensor. The relationship can be expressed as:

$$g_m = \left(\frac{\partial I_d}{\partial V_{g,ext}}\right)_{V_d}. \quad \text{(S7)}$$

where g_m is the transconductance of a FET.

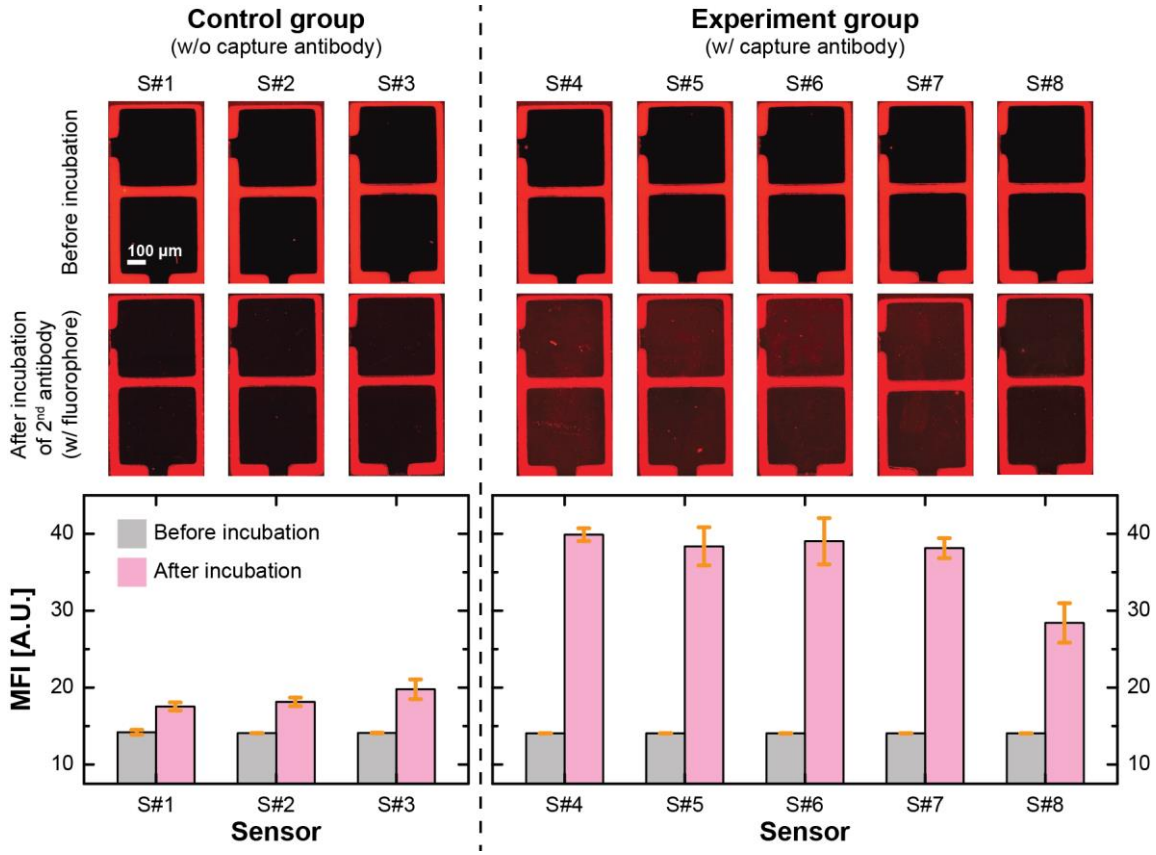

Supplemental Figure 3. The fluorescent images (top) and the measured fluorescence intensities (bottom). The error bars represent one standard deviation of fluorescent uncertainties measured from 8 subregions within a sensor.

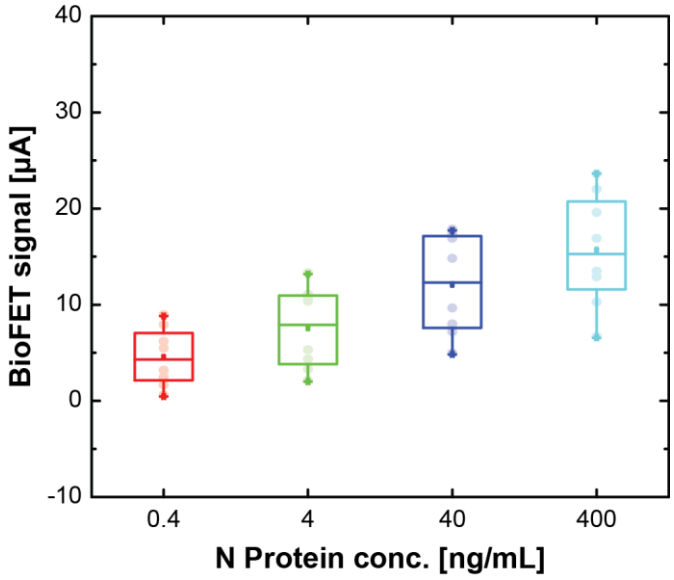

Supplemental Figure 4. The box chart showing sensor-to-sensor variation of BioFET measurements in PBS. Measured data were collected from 3 different sensor sticks that had 7 working sensors in total.

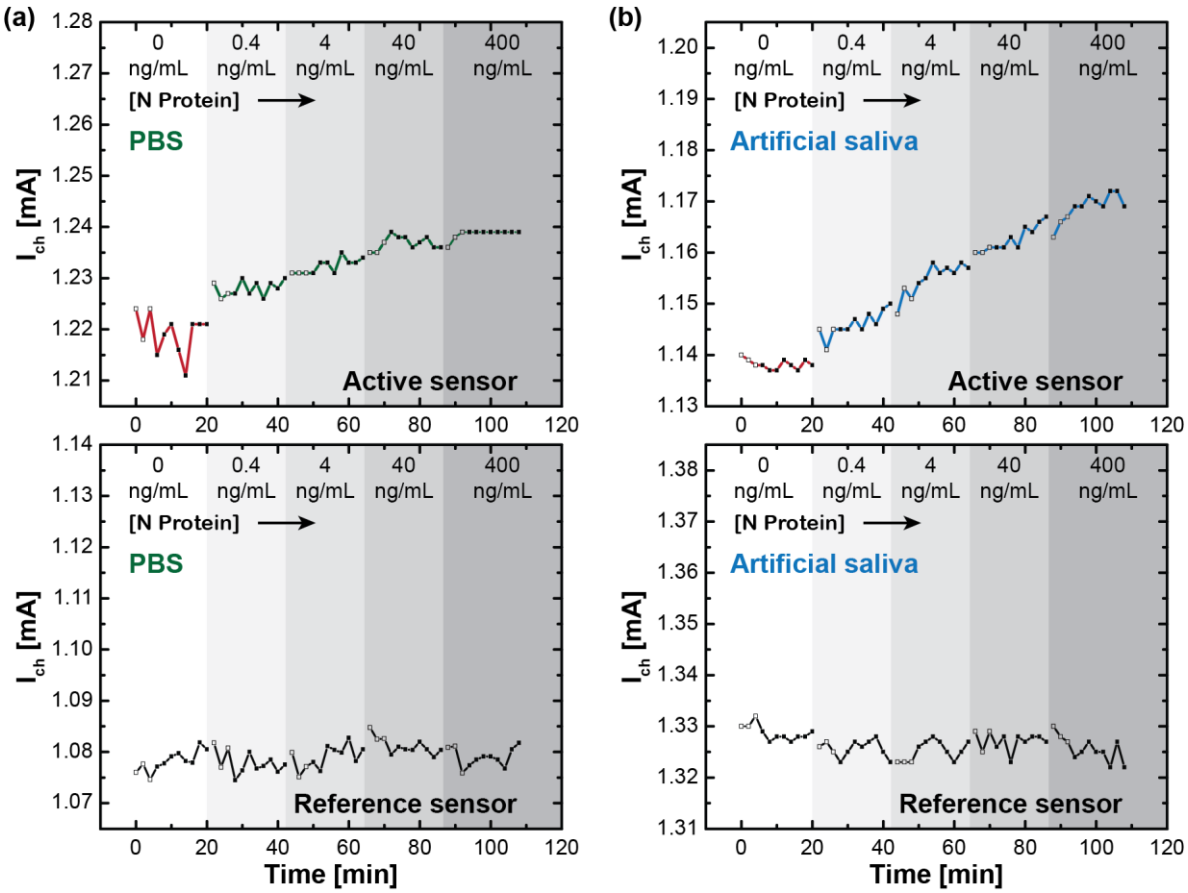

Supplemental Figure 5. Real-time results of COVID-19 antigen tests in **(a)** 1× PBS and **(b)** artificial saliva.

References

[1] K.B. Oldham, A Gouy–Chapman–Stern model of the double layer at a (metal)/(ionic liquid) interface, J. Electroanal. Chem. 613 (2008) 131–138. https://doi.org/10.1016/j.jelechem.2007.10.017.

[2] H. Zhang, A.A. Hassanali, Y.K. Shin, C. Knight, S.J. Singer, The water–amorphous silica interface: Analysis of the Stern layer and surface conduction, J. Chem. Phys. 134 (2011) 024705. https://doi.org/10.1063/1.3510536.

[3] M. Elimelech, J. Gregory, X. Jia, R.A. Williams, Chapter 2 - Electrical properties of interfaces, in: Part. Depos. Aggreg., Butterworth-Heinemann, Woburn, MA, USA, 1995: pp. 9–32. https://doi.org/10.1016/B978-075067024-1/50002-9.

[4] P. Bergveld, ISFET, theory and practice, in: IEEE Sens. Conf. Tor., 2003: pp. 1–26.

[5] G. Sposito, Gouy-Chapman Theory, in: W.M. White (Ed.), Encycl. Geochem. Compr. Ref. Source Chem. Earth, Springer International Publishing, Cham, 2018: pp. 623–628. https://doi.org/10.1007/978-3-319-39312-4_50.